

Semi-Analytical 3D Force Calculation of an Ironless Cylindrical Permanent Magnet Actuator for Magnetic Levitation Systems

Mousa Lahdo^{1,2}, Tom Ströhla², and Sergej Kovalev¹

¹ Department of Informatics, Electrical Engineering and Mechatronics
University of Applied Sciences Mittelhessen, Friedberg, 61169, Germany
mousa.lahdo@iem.thm.de, sergej.kovalev@iem.thm.de

² Department of Mechatronics
Ilmenau University of Technology, Ilmenau, 98693, Germany
tom.stroehla@tu-ilmenau.de

Abstract — The semi-analytical calculation of magnetic forces is currently an interesting alternative to the time-consuming three-dimensional finite-element modeling (3D-FEM) due to its high accuracy and low computational cost. This paper presents novel equations for determining the magnetic forces of a cylindrical permanent magnet actuator used in high precision magnetic levitation positioning systems. Compared to the already available equations in literature, these equations consider the magnetic forces as a function of the current magnet position. Moreover, these equations are also suitable for designing and analyzing the cylindrical permanent magnet actuator. The results of our force equations and the verification by 3D-FEM and measurements are presented in this paper.

Index Terms — Cylindrical permanent magnet actuator, electromagnetic analysis, Lorentz force, magnetic levitation.

I. INTRODUCTION

Magnetic levitation is a key technology used in order to achieve vacuum compatible high precision positioning systems since friction, backlash, and wear are eliminated. Positioning systems based on magnetic levitation are characterized by a simple compact structure with highest positioning accuracy, excellent repeatability and high control bandwidth. Thus, six degrees-of-freedom (6-DoF) magnetic levitation positioning systems are currently investigated and developed for applications in the semiconductor industry, nanotechnology or microscopy, where highest dynamics, highest precision and absolutely friction-free operation are desired [1-5].

Due to the non-linear current-force and position-force relation in reluctance actuators, which complicates controller design, most existing solutions of magnetic levitation positioning systems are based on ironless

actuators which use Lorentz forces to levitate and drive the moving element (mover).

The main advantages of ironless actuators based on Lorentz forces are its inherent linear relation between the currents and forces and its high positioning accuracy [6-7].

Designing, analyzing and optimizing such ironless high precision positioning systems require electromagnetic models that are very fast and accurate. Three-dimensional finite element modeling (3D-FEM) is often used for the calculation of magnetic fields and forces of such systems because they provide a very accurate solution. However, 3D-FEM is not suitable for designing and optimizing such systems because of its extremely high computation time. Thus, other calculation approaches are needed. A very fast and accurate alternative to the conventional 3D-FEM modeling is a semi-analytical-based modeling approach. The semi-analytical approach describes the magnetic fields and forces as a function of physical parameters, e.g., magnet and coil dimensions and thus, provides a good insight in the physical system properties. Moreover, for the design and optimization of electromagnetic actuators, such equations are more efficient compared to 3D-FEM. Beyond that, researchers do not always have the possibility to use a cost-intensive 3D-FEM software, therefore, a precise semi-analytical equation is a good alternative since it can be implemented in every mathematical program.

Due to these reasons, many researchers calculate the magnetic fields and forces in electromagnetic systems semi-analytically instead of using 3D-FEM. This can be seen by the huge number of publications dealing with semi-analytical calculation of magnetic fields and forces [8-14]. For instance, in a recent publication, [15] derives analytical expressions in order to optimize a magnetically levitated planar motor. The analytical calculation of repulsive levitation forces between Halbach arrays and

magnetic guiding coils in high precision magnetic levitation systems is presented in [16]. An overview of different analytical calculation methods is given in [17].

In high precision magnetic levitation systems, ironless rectangular coils [18], square coils [19] or circular coils [20] are commonly used in order to generate repulsive levitation forces. Until now, many papers published in literature deal with the semi-analytical force calculation between a cuboidal permanent magnet and a rectangular [21] or square air-core coil [22]. The derived force equations for the rectangular and square coils consider also the position dependence of the magnetic forces and thus provide the basis for fast and accurate analysis and design tools [21-22]. Moreover, these equations can also be used for the derivation of model-based commutation algorithms as well as real-time motion control of magnetic levitation positioning systems [23-25].

The semi-analytical force calculation between circular air-core coils and cylindrical permanent magnets are also known, but these equations are only valid in cases where the center axis of cylindrical magnet and the circular coil are coaxial [26-29]. However, in 6-DoF magnetic levitation system, a movement of the permanent magnet in the horizontal plane is indispensable, i.e., the center of the cylindrical magnet and the circular coil are not coaxial and thus the force equations known in literature are not valid for the non-coaxial case. Since this case has not yet been investigated in the context of high precision magnetic levitation systems, it is rare to find equations which consider the Cartesian magnetic force components (F_x, F_y, F_z) as a function of the current mover position (x_p, y_p). Previous efforts to determine the magnetic forces between a circular coil and a cylindrical permanent magnet are mostly done by experiments [30] or by 3D-FEM [31].

As such, this paper aims to provide a semi-analytical calculation of the repulsive magnetic levitation force between a cylindrical moving magnet and a stationary circular coil.

Moreover, the calculation of the destabilizing propulsion forces is also presented. The main contributions of this paper are new semi-analytical expressions which consider the Cartesian magnetic force components as a function of the current mover position.

This paper is organized as follows: Section II explains briefly the force generation principle of the cylindrical magnet actuator. The generation and calculation of the levitation and propulsion force as a function of the mover position is described in Section III. In Section IV, the calculated levitation and propulsion forces using the new expressions are compared with the calculated forces using 3D-FEM and with our measured forces obtained from the prototype. Section V concludes this paper.

II. ANALYSIS AND MAGNETIC FIELD CALCULATION

In high precision magnetic levitation systems, the active magnetic guidance coil has a significant weight that must be levitated, e.g. the weight of the magnet, the plate to which it is fixed and the weight of an additional payload. Hence, the calculation of the levitation forces is an important task in such positioning systems. Compared with cost-intensive experiments and time-consuming 3D-FEM software, the proposed approach in this paper ensures the possibility of calculating quickly the levitation force as a function of the coil and magnet dimensions and thus is suitable for parameter studies.

A. Force generation principle

The permanent magnet actuator usually used in magnetic levitation systems in order to generate the repulsive levitation force can be seen in Fig. 1. It consists of a fixed circular air-core coil and a moving cylindrical permanent magnet.

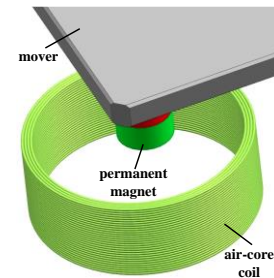


Fig. 1. Cylindrical permanent magnet actuator.

However, such topologies based on static magnetic forces are inherently unstable. This means that the permanent magnet actuator generates, in addition to the desired stable repulsive levitation force, an undesired destabilizing propulsion force that tends to push the permanent magnet laterally away from the equilibrium position. Figure 2 shows a more detailed illustration of this unstable behavior.

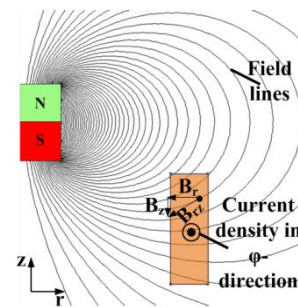


Fig. 2. Generated force components by the permanent magnet actuator.

As can be seen from this figure, the magnetic field generated by the cylindrical permanent magnet creates flux density components in the r - and z -directions. The interaction of the r -component of the magnetic flux density with the φ -component of the current density in the circular coil generates a levitation force in the z -direction.

An equilibrium position occurs, when the repulsive levitation force in $+z$ -direction exactly compensates the gravitational force of the mover in the $-z$ -direction. As a result, this equilibrium position is stable, i.e., the motion of the mover along the z -direction is stable. This is because as the air gap increases, the generated repulsive levitation force decreases. Thus, the gravitational force restore the mover in the equilibrium position. Nevertheless, the z -component of the magnetic flux density generates with the same current density in the coil a destabilizing propulsion force in the r -direction. This instability is consistent with Earnshaw's theorem predicted by S. Earnshaw in the early 1800 and Braunbek's theorem, which states that a stable levitation based only on static magnetic forces between coils and permanent magnets is never stable in all directions simultaneously [32,34]. Thus, this destabilizing force must be compensated by additional propulsion actuators in order to restore the lateral stability and to move and position the mover simultaneously as it is proposed among others in [1], [19],[20],[22],[29],[30],[31].

Consequently, a stable levitation can only be achieved with additional propulsion actuators in combination with a control system.

The total force which acts on the fixed circular air-core coil can be calculated using the Lorentz force formula:

$$\mathbf{F} = \int_V \mathbf{J} \times \mathbf{B} dV, \quad (1)$$

which states that the Lorentz force is the volumetric integral of the cross product of the current density \mathbf{J} in the coil with the external magnetic flux density \mathbf{B} generated by the permanent magnet over the whole volume $dV = dx dy dz$ of the coil. However, since the Lorentz force formula can only applied to the current carrying coil, the permanent magnet will experience according to Newton's third law the same force in opposite direction (*action = reaction*).

B. Calculation of the magnetic flux density

The first important step for the prediction of the Lorentz force according to (1) is the calculation of the magnetic flux density of the permanent magnet inside the coil volume. In literature, many 3D-field equations are

presented for different permanent magnet shapes. These equations are based on either the current sheet model or on the surface charge model [33]. Both approaches can be derived from the Maxwell equations under the assumption that the relative permeability $\mu_r = 1$. Moreover, both allow an extremely accurate and fast field calculation, provide a good insight into the system properties and leads to the same results in free space [28].

In this paper, the magnetic flux density for an axial magnetized permanent magnet with a uniform magnetization is determined using the surface charge model and this is given by [22]:

$$\mathbf{B} = \frac{\mu_0}{4\pi} \nabla_r \oint_S \frac{\mathbf{M}(\mathbf{r}') \cdot \mathbf{n}}{|\mathbf{r} - \mathbf{r}'|} dS, \quad (2)$$

where $\mathbf{M}(\mathbf{r}')$ is the magnetization of the permanent magnet, \mathbf{n} is the normal vector on the surface, μ_0 is the vacuum permeability, S is the surface of the permanent magnet, ∇_r is the vector operator, \mathbf{r} describes the position where the field is evaluated and \mathbf{r}' describes the position of the permanent magnet.

III. FORCE CALCULATION

Using (2) and inserting into (1), the total force can be generally written as:

$$\mathbf{F} = \int_V \mathbf{J} \times \left(\frac{\mu_0}{4\pi} \nabla_r \oint_S \frac{\mathbf{M}(\mathbf{r}') \cdot \mathbf{n}}{|\mathbf{r} - \mathbf{r}'|} dS \right) dV. \quad (3)$$

This quintuple integral expression can be generally used in order to calculate the total force generated between a permanent magnet and an air-core coil. For the circular air-core coil, the current density in a cylindrical coordinate system only has a component in the tangential direction. Hence, in order to obtain a formula for the levitation force, only the flux density component in the radial direction is needed because only this component is responsible for the levitation force generation. Therefore, this radial component is given as:

$$B_r = \frac{\mu_0}{4\pi} \frac{\partial}{\partial r} \oint_S \frac{\mathbf{M}(\mathbf{r}') \cdot \mathbf{n}}{|\mathbf{r} - \mathbf{r}'|} dS. \quad (4)$$

Furthermore, if we assume that the current density is uniform and constant:

$$J_\varphi = \frac{N_c \cdot I_c}{(r_a - r_i) \cdot h_c}, \quad (5)$$

where N_c is the number of coil turns, I_c the current through the coil, $(r_a - r_i) \cdot h_c$ the cross sectional area of the coil and under consideration of the parameters shown also in Fig. 3, the expression for the levitation force F_z at the magnet position $x = y = 0$ can be simplified to a scalar function in z -direction:

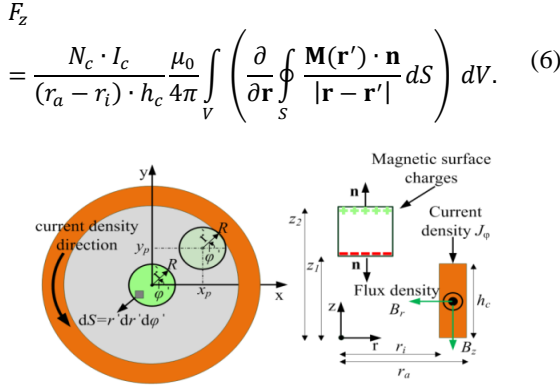


Fig. 3. Top view (left) and side view (right) of the permanent magnet actuator.

The difference vector $\xi_\beta = |\mathbf{r} - \mathbf{r}'|$ expressed in cylindrical coordinates using the relation $\mathbf{r} = \{x, y, z\} = \{r \cos \varphi, r \sin \varphi, z\}$ and $\mathbf{r}' = \{x', y', z'\} = \{r' \cos \varphi', r' \sin \varphi', z'\}$ yields:

$$\begin{aligned} \xi_\beta &= |\mathbf{r} - \mathbf{r}'| \\ &= \sqrt{(x - x')^2 + (y - y')^2 + (z - z')^2} \\ &= \sqrt{r^2 + r'^2 - 2rr' \cos(\varphi - \varphi') + (z - z')^2}. \end{aligned} \quad (7)$$

In addition to that, if the infinitesimal volume element dV as well as the infinitesimal surface element dS is also expressed in cylindrical coordinates as $dV = r dr d\varphi dz$ and $dS = r' dr' d\varphi'$ respectively, and under consideration of Fig. 3, the levitation force F_z now becomes:

$$\begin{aligned} F_z &= \frac{N_c \cdot I_c}{(r_a - r_i) \cdot h_c} \frac{\mu_0 M}{4\pi} \int_0^{h_c} \int_0^{2\pi} \int_{r_i}^{r_a} \frac{\partial}{\partial r} \int_0^{2\pi} \int_0^R \left(\frac{r'}{\xi_2} - \frac{r'}{\xi_1} \right) \\ &\quad \cdot dr' d\varphi' \cdot r dr d\varphi dz. \end{aligned} \quad (8)$$

However, this equation allows determining the levitation force only if the center of the permanent

magnet is coaxial with the center of the circular coil as can be seen in Fig. 3.

Despite this, in 6-DoF magnetic levitation system, the magnet moves in the horizontal plane x_p and y_p from the central position (Fig. 3). Therefore, the analytical equation must consider the actual mover position (x_p, y_p) over the whole travel range.

This can be done by modifying the integrand of (6) with the relationship $\mathbf{r}' = \{x', y', z'\} = \{x_p + r' \cos \varphi', y_p + r' \sin \varphi', z'\}$ as shown in the final form (9) at the bottom of this page.

At this point, it should be noted that the derivation of semi-analytical expressions for the destabilizing forces in the horizontal direction can be done in the same manner. Thus, the force equations for the Cartesian force components in the x - and y -direction can be derived in the final form as shown in (11) and (12), respectively.

Based on the derived expressions, which are easily implemented in MATLAB, and under consideration of the parameters and dimensions shown in Table 1, the levitation and the destabilizing propulsion forces can be calculated at every value of x_p and y_p in millimeters in the horizontal plane $(x_p, y_p) \in \mathbb{R}$.

Table 1: Dimensions and parameters for the levitation force calculation

Parameter	Symbol	Value	Unit
Number of turns	N_c	200	
Current	I_c	1	A
Remanence of PM	$\mu_0 M$	1.44	Vs/m ²
Coil height	h_c	24	mm
Magnet radius	R	10	mm
Coil inner side	r_i	23.5	mm
Coil outer side	r_a	33.5	mm
Neg. magnetic charges height	z_1	26	mm
Pos. magnetic charges height	z_2	31	mm

$$F_z(x_p, y_p) = \frac{N_c \cdot I_c}{(r_a - r_i) \cdot h_c} \frac{\mu_0 M}{4\pi} \int_0^{h_c} \int_0^{2\pi} \int_{r_i}^{r_a} \frac{\partial}{\partial r} \int_0^{2\pi} \int_0^R \left(\sum_{\beta=1}^2 \frac{(-1)^\beta \cdot r'}{Y_\beta} \right) dr' d\varphi' \cdot r dr d\varphi dz, \quad (9)$$

where

$$Y_\beta = \sqrt{\xi_\beta^2 + x_p^2 + y_p^2 - 2r(x_p \cos(\varphi) + y_p \sin(\varphi)) + 2r'(x_p \cos(\varphi') + y_p \sin(\varphi'))}, \quad (10)$$

$$F_x(x_p, y_p) = \frac{N_c \cdot I_c}{(r_a - r_i) \cdot h_c} \frac{\mu_0 M}{4\pi} \int_0^{h_c} \int_0^{2\pi} \int_{r_i}^{r_a} \frac{\partial}{\partial z} \int_0^{2\pi} \int_0^R \left(\sum_{\beta=1}^2 \frac{(-1)^\beta \cdot r' \cos(\varphi)}{Y_\beta} \right) dr' d\varphi' \cdot r dr d\varphi dz, \quad (11)$$

$$F_y(x_p, y_p) = \frac{N_c \cdot I_c}{(r_a - r_i) \cdot h_c} \frac{\mu_0 M}{4\pi} \int_0^{h_c} \int_0^{2\pi} \int_{r_i}^{r_a} \frac{\partial}{\partial z} \int_0^{2\pi} \int_0^R \left(\sum_{\beta=1}^2 \frac{(-1)^\beta \cdot r' \sin(\varphi)}{Y_\beta} \right) dr' d\varphi' \cdot r dr d\varphi dz. \quad (12)$$

Figures 4 to 6 show exemplary the calculation of the force components in the horizontal square plane from -10 mm to $+10$ mm.

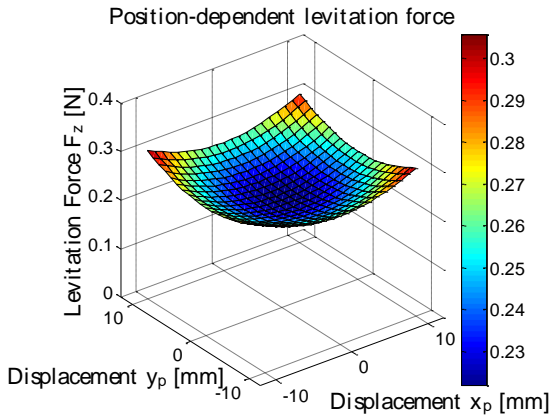


Fig. 4. F_z as a function of the mover position (x_p, y_p) .

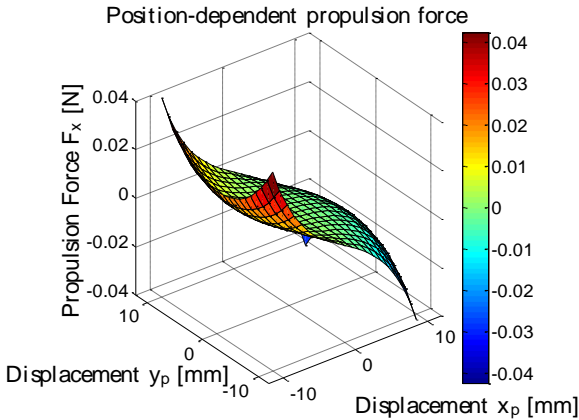


Fig. 5. F_x as a function of the mover position (x_p, y_p) .

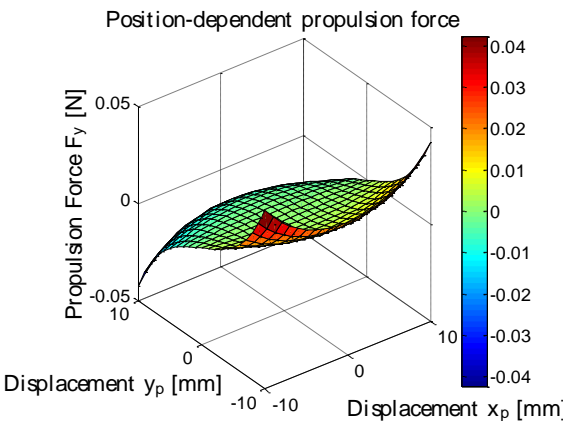


Fig. 6. F_y as a function of the mover position (x_p, y_p) .

As can be seen in these figures, all force components are strongly position-dependent due to the non-uniform magnetic field generated by the cylindrical permanent magnet. The force that the circular coil can generate in

order to levitate the moving element is minimal at the central position, i.e., $x_p = y_p = 0$. However, this levitation force increases when the magnet deviates laterally away from the central position. The same behavior shows also the destabilizing force curves.

In general, the derived force equations are semi-analytical, i.e., after two consecutive analytical integrations and one analytical derivation with the Symbolic Math Toolbox of MATLAB, it is difficult to express the remaining expression in an analytical form. Therefore, the remaining analytical expression must be converted to a function handle using *matlabFunction* and calculated numerically using the intern numerical integration function *integral3*. In order to simplify the calculation procedure, a MATLAB program is written which contains the analytical and numerical calculation.

IV. VERIFICATION OF THE EQUATIONS

In order to verify the derived equations, a 3D-FEM model of the cylindrical permanent magnet actuator has been implemented in Maxwell 3D. Moreover, a prototype of the permanent magnet actuator was developed in order to measure the generated forces using a precision load cell. The 3D-FEM model and the prototype can be seen in Fig. 7.

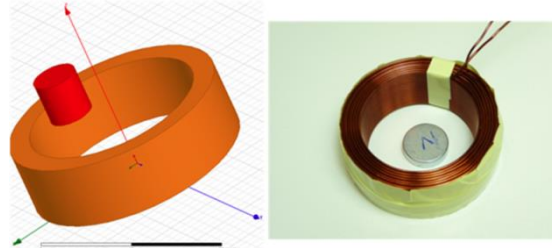


Fig. 7. 3D-FEM model (left) and prototype of the permanent magnet actuator (right).

The permanent magnet used in this study is a neodymium–iron–boron (*NdFeB*) magnet, which has a relative square hysteresis loop with high coercivity and high remanence [33].

Figure 8 (a) compares the current-levitation force curve using the derived equation (9) with the measured results and with 3D-FEM in cases where the mover is at the centered position and the air gap is equal to $z=1$ mm.

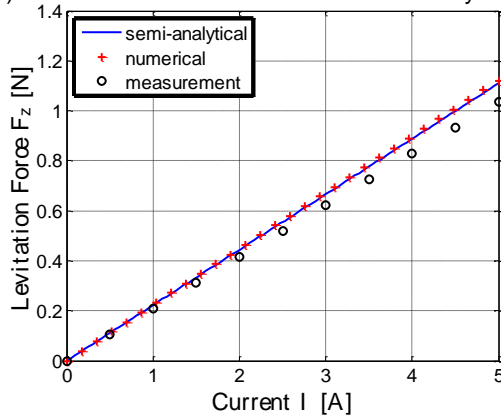
As can be observed, all curves show a linear relation between the current and the levitation force. This linear relation is as expected, because according to (9), the coil current is directly proportional to the levitation force. A further explanation for the linear relationship is that there are no ferromagnetic materials that can cause a non-linear relationship due to hysteresis and saturation, i.e., from an electromagnetic point of view it is a linear system.

Compared to reluctance actuators, where the

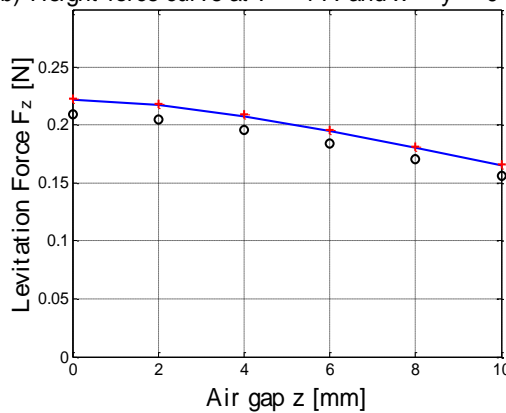
levitation force decreases rapidly as the air gap grows the levitation force in the ironless actuator decreases slightly (Fig. 8 (b)). This advantageous characteristic allows compensating the force variation along the z -axes easily using control algorithms.

Figure 8 (c) shows the influence of the horizontal movement on the levitation force. It can be observed that the force increases when the magnet deviates laterally from the central position (similar to Fig. 5 and Fig. 6).

a) Current-force curve at $z = 1$ mm and $x = y = 0$ mm



b) Height-force curve at $I = 1$ A and $x = y = 0$ mm



c) Displacement-force curve at $z = 1$ mm, $y_p = 0$ mm and $I = 1$ A

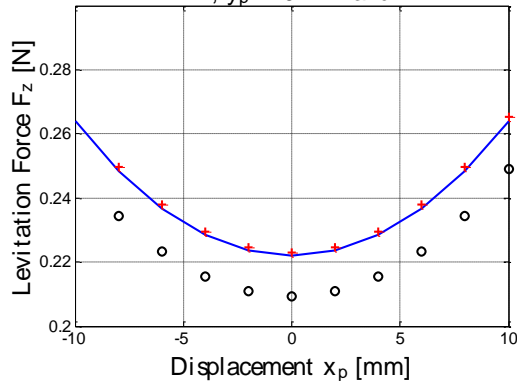


Fig. 8. Measured and calculated curves of the permanent magnet actuator.

If the center of the moving permanent magnet is coaxial with the center of the circular coil, then the destabilizing force components in the x - and y -direction are zero due to symmetry. However, when the magnet moves from the central position, it experiences also in addition to the levitation force a destabilizing (propulsion) force that tends to push the permanent magnet laterally away from the center position. This unstable behavior can be seen in Fig. 9.

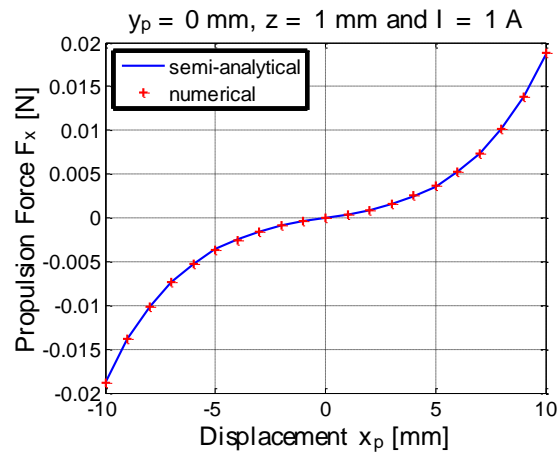


Fig. 9. Destabilizing force F_x .

Since the magnitude of the destabilizing force is too small to measure accurately, we verified the derived equation only with 3D-FEM in case the magnet moves only along the x -axes (the y -component of the force is zero in this case).

As evident from all the figures, there is an excellent agreement between the calculated forces using the derived equations (9)-(12) and 3D-FEM as well as the measurements.

The maximum error between the solutions of 3D-FEM and our equations is below 1%, whereas the maximum error between our equation and the measurements is below 6%. Apart from the manufacturing tolerances in the magnet and coil dimensions as well as the mechanical and mounting tolerances of our experimental setup, the main reason for the observed error is that our equation assumes an ideal magnet with $\mu_r = 1$. However, the magnetization of the magnet is not perfectly uniform and the relative permeability of real available $NdFeB$ permanent are close to 1 ($\mu_r = 1.05 \dots 1.1$) with 5% tolerance on magnetization strength [33]. In [21], it is shown that the assumption of an ideal magnet cause an error of approximately 3%.

Despite this, our proposed equations can be used for studying the characteristics of the permanent magnet actuator and these results can be used in the design and real-time control for high precision 6-DoF magnetic levitation systems, e.g., shown in [30] and [31]. Compared to 3D-FEM software, the calculation of the magnetic

fields and the generated forces as well as the optimization of the permanent magnet actuator can be obtained in a very short calculation time.

V. CONCLUSION

In this paper, new and compact equations for calculating the magnetic force components of a cylindrical permanent magnet for ironless magnetic levitation systems were derived and presented. These equations can help to evaluate quickly and precisely the performance of the proposed actuator. Moreover, the derived equations consider also the position-dependent characteristic of the force components. They provide an interesting alternative to 3D-FEM software since they are also accurate and easily applicable for researchers. The semi-analytical results are verified with 3D-FEM and with our prototype which illustrate the accuracy of these force equations.

REFERENCES

- [1] S. Verma, H. Shakir and W.-J. Kim, "Novel electro-magnetic actuation scheme for multiaxis nano-positioning," *IEEE Trans. Magn.*, vol. 42, no. 8, pp. 2052-2062, May 2006.
- [2] X. Lu and I. Usman, "6D direct-drive technology for planar motion stages," *CIRP Ann.-Manuf. Technol.*, vol. 61, no. 1, pp. 359-362, 2012.
- [3] W.-J. Kim and D. L. Trumper, "High-precision magnetic levitation stage for photolithography," *Precis. Eng.*, vol. 22, no. 2, 1998, pp. 66-77, Apr. 1998.
- [4] J. W. Jansen, C. M. M. van Lierop, E.A. Lomonova and A. J. A. Vandanput, "Magnetically levitated planar actuator with moving magnets," *IEEE Trans. Ind. Appl.*, vol. 44, no. 4, pp. 1108-1115, July 2008.
- [5] L. Guo, H. Zhang, M. Galea, J. Li, W. Lu, and C. Gerada, "Analysis and design of a magnetically levitated planar motor with novel multilayer windings," *IEEE Trans. Magn.*, vol. 51, no. 8, art. no. 8106909, Aug. 2015.
- [6] A. C. P. de Klerk, G. Z. Angelis, and J. van Eijk, "Design of a next generation 6 Dof stage for scanning application in vacuum with nanometer accuracy and mGauss magnetic stray field," *Proc. Annu. Meeting-Amer. Soc. Precis. Eng.*, pp. 60-63, 2004.
- [7] T. J. Teo, I.-M. Chen, G. Yang, and W. Lin, "Magnetic field modeling of a dual-magnet configuration," *J. Appl. Phys.*, vol. 102, art. no. 074924, 2007.
- [8] M. Lahdo, T. Ströhla, and S. Kovalev, "Magnetic propulsion force calculation of a 2-DoF large stroke actuator for high-precision magnetic levitation system," *ACES Journal*, vol. 32, no. 8, Aug. 2017.
- [9] A. Shiri and A. Shoulaie, "Calculation of the magnetic forces between planar spiral coils using concentric rings," *ACES Journal*, vol. 25, no. 5, May 2010.
- [10] R. Muscia, "Magneto-mechanical model of passive magnetic axial bearings versus the eccentricity error - Part 1: physical mathematical model," *ACES Journal*, vol. 32, no. 8, Aug. 2017.
- [11] J. L. G. Janssen, J. J. H. Paulides, and E. A. Lomonova, "3-D analytical calculation of the torque between perpendicular magnetized magnets in magnetic suspensions," *IEEE Trans. Magn.*, vol. 47, no. 10, pp. 4286-4289, Oct. 2011.
- [12] S. Wu, S. Zuo, X. Wu, F. Lin, and J. Shen, "Magnet modification to reduce pulsating torque for axial flux permanent magnet synchronous machines," *ACES Journal*, vol. 31, no. 3, Mar. 2016.
- [13] R. Bjork, A. Smith, and C. R. H. Bahl, "Analysis of the magnetic field, force and torque for two-dimensional Halbach cylinders," *J. Magn. Mater.*, vol. 322, no. 1, pp. 131-141, 2010.
- [14] T. R. N. Mhiócháin, D. Weaire, S. M. McMurry, and J. M. D. Coey, "Analysis of torque in nested magnetic cylinders," *J. Appl. Phys.*, vol. 86, no. 11, pp. 3412-3424, 1999.
- [15] L. Guo, H. Zhang, M. Galea, J. Li, and C. Gerada, "Multiobjective optimization of a magnetically levitated planar motor with multilayer windings," *IEEE Trans. Ind. Elect.*, vol. 63, no. 6, pp. 3522-3532, June 2016.
- [16] J. W. Jansen, J. L. G. Janssen, J. M. M. Rovers, J. J. H. Paulides, and E. Lomonova, "(Semi-) analytical models for the design of high precision permanent magnet actuators," *Int. Compomag. Soc. Newslett.*, vol. 16, no. 02, pp. 4-17, 2009.
- [17] J. W. Jansen, J. P. C. Smeets, T. T. Overboom, J. M. M. Rovers, and E. A. Lomonova, "Overview of analytical models for the design of linear and planar motors," *IEEE Trans. Magn.*, vol. 50, no. 11, art. no. 8206207, Dec. 2014.
- [18] H. Zhang, B. Kou, H. Zhang, and Y. Xi, "A three-degree-of-freedom short-stroke Lorentz-force-driven planar motor using a Halbach permanent magnet array with unequal thickness," *IEEE Trans. Ind. Elect.*, vol. 62, no. 6, pp. 3640-3650, June 2015.
- [19] K. S. Jung and Y. S. Baek, "Study on a novel contact-free planar system using direct drive DC coils and permanent magnets," *IEEE/ASME Trans. Mech.*, vol. 7, no. 2, pp. 35-43, Mar. 2002.
- [20] M.-Y. Chen, T.-B. Lin, S.-K. Hung, and L.-C. Fu, "Design and experiment of a macro-micro planar maglev positioning system," *IEEE Trans. Ind. Elect.*, vol. 59, no. 11, pp. 4128-4139, Nov. 2012.
- [21] J. M. M. Rovers, J. W. Jansen, and E. A. Lomonova, "Analytical calculation of the force between a rectangular coil and a cuboidal permanent magnet," *IEEE Trans. Magn.*, vol. 46, no. 6, pp. 1656-1659, June 2010.
- [22] M. Lahdo, T. Ströhla, and S. Kovalev, "Repulsive

magnetic levitation force calculation for a high precision 6-DoF magnetic levitation positioning system,” *IEEE Trans. Magn.*, vol. 53, no. 3, Mar. 2017.

- [23] J. Peng, Y. Zhou, and G. Liu, “Calculation of a new real-time control model for the magnetically levitated ironless planar motor,” *IEEE Trans. Magn.*, vol. 49, no. 4, pp. 1416-1422, Apr. 2013.
- [24] F. Liu, M. Zhang, Y. Zhu, and C. Hu, “A real-time model of ironless planar motors with stationary circular coils,” *IEEE Trans. Magn.*, vol. 51, no. 7, art. no. 8203110, July 2015.
- [25] C. M. M. van Lierop, J. W. Jansen, A. A. H. Damen, E. A. Lomonova, P. P. J. van den Bosch, and A. J. A. Vandenput, “Model-based commutation of a long-stroke magnetically levitated linear actuator,” *IEEE Trans. Ind. Appl.*, vol. 45, no. 6, pp. 1982-1990, Nov./Dec. 2009.
- [26] S. Verma, W.-J. Kim, and H. Shakir, “Multi-axis maglev nanopositioner for precision manufacturing and manipulation applications,” *IEEE Trans. Ind. Appl.*, vol. 41, no. 5, pp. 1159-1167, Sep./Oct. 2009.
- [27] W. Robertson, B. Cazzolato, and A. Zander, “Axial force between a thick coil and a cylindrical permanent magnet: Optimizing the geometry of an electromagnetic actuator,” *IEEE Trans. Magn.*, vol. 48, no. 9, pp. 2479-2487, Sep. 2012.
- [28] R. Ravaut, G. Lemarquand, S. Babic, V. Lamarquand, and C. Akyel, “Cylindrical magnets and coils: Fields, forces, and inductances,” *IEEE Trans. Magn.*, vol. 46, no. 9, pp. 3585-3590, Sep. 2010.
- [29] H. Zhang, B. Kou, Y. Jin, and H. Zhang, “Modeling and analysis of a new cylindrical magnetic levitation gravity compensator with low stiffness for the 6-DOF fine stage,” *IEEE Trans. Ind. Elect.*, vol. 62, no. 6, pp. 3629-3639, June 2015.
- [30] P. Berkelman and M. Dzadoovsky, “Magnetic levitation over large translation and rotation ranges in all directions,” *IEEE/ASME Trans. Mech.*, vol. 18, no. 1, pp. 44-52, Feb. 2013.
- [31] Y. C. Lai, Y. L. Lee, and J. Y. Yen, “Design and servo control of a single-deck planar maglev stage,” *IEEE Trans. Magn.*, vol. 43, no. 6, pp. 2600-2602, June 2007.
- [32] S. Earnshaw, “On the nature of the molecular forces which regulate the constitution of the luminiferous ether,” *Trans. Cambridge Philos. Soc.*, vol. 7, pp. 97-112, Mar. 1839.
- [33] E. P. Furlani, *Permanent Magnet and Electro-mechanical Devices: Materials, Analysis and Application*. 6th Edition, Academic Press, London, 2001.
- [34] W. Braunbek, “Freischwebende Körper im elektrischen und magnetischen Feld,” *Z. Physik*, vol. 112, pp. 753-763, 1939.



Mousa Lahdo received the diploma degree in Electrical Engineering from the University of Applied Sciences Mittelhessen in Friedberg, Germany, in 2012. Since 2015, he is a Research Associate and Ph.D. student at the Department of Mechatronics, Ilmenau University of Technology. His current research interests include magnetic bearings and magnetic levitation systems and novel integrated electro-mechanical actuators and motors.



Tom Ströhla researches at the Department of Mechatronics, Ilmenau University of Technology. He teaches Electrical Drive Systems as well as Mechanical and Fluid Actuators. He completed his Ph.D. on the subject of model-based design of electromagnets and he was involved in the development of the draft for the software SESAM. In numerous research and industrial projects, he gained experience in the design of electromagnetic drives and the magnetic measurement technology. He is co-author of several books on electromagnets and theoretical electrical engineering.



Sergej Kovalev is Professor for Electrical Drives, Electrical Engineering and Measurement Systems at the University of Applied Sciences in Friedberg, Germany, since 2012. He enrolled as a Ph.D. candidate in the Mechatronics Department at Technical University Ilmenau, Germany, in 1995 and received his Ph.D. degree in 2001. He has 14 years industrial experience in the R&D departments at different firms in Germany. His research interest is the mechatronics of precision engineering, especially direct drives.